The observed currents in summer in the Bohai Sea[*]

QIAO Lulu (乔璐璐)[†,††,**], BAO Xianwen (鲍献文)[†,††], WU Dexing (吴德星)[†,††]

[†]College of Physical and Environmental Oceanography, Ocean University of China, Qingdao 266100, China

[††]Key Laboratory of Physical Oceanography, Ministry of Education, Qingdao 266003, China

Abstract   A harmonic method was used to analyze the tidal currents observed in summer at 11 stations made from 1996 to 2001 in the Bohai Sea, China. Data was compared among different instruments and intervals. Elliptic elements were calculated based on harmonic constants, of which vertical distributions of the maximum speed and rotation direction were discussed for understanding the characteristics of diurnal and semi-diurnal tidal current components. The results indicate that the maximum speed of M_2 tidal current component is much larger than that of K_1; the rotation direction of M_2 tidal current constituent is clockwise in the central part of the Bohai Sea and in the Laizhou Bay, but anticlockwise in the Liaodong Bay and Bohai Bay. For K_1 tidal current constituent, it is clockwise in the central Bohai Sea but anti-clockwise in the Laizhou Bay and Liaodong Bay. The tidal currents in most stations in the Bohai Sea were regular semidiurnal except for those in the central Bohai Sea, being irregular semidiurnal.

Keyword: observed tidal current; the Bohai Sea; harmonic analysis

1 INTRODUCTION

Tidal current, one of the most important dynamic phenomena in the Bohai Sea, has been of great concern to scientists. Although there are many numerical studies (Fang and Yang, 1985; Dou et al., 1993; Huang, et al., 1999; Bao et al., 2000; Wan et al., 2003; Wu et al., 2004; Wei et al., 2004; Li et al., 2005), few analyses on observed data have been conducted for the Bohai Sea (Kuang et al., 1991; Lou et al., 2002; Yu et al., 2002). Numerical modeling is an important tool for understanding in depth the tidal currents in the Bohai Sea. However, some still argued on different model results that caused probably by lacking enough observed data. Furthermore, data analysis of a single station (Kuang et al., 1991; Lou et al., 2002; Yu et al., 2002) is useful to get the local picture but entire understanding. Therefore, in this study, some tidal current data observed in summer covering nearly the whole Bohai Sea were analyzed with harmonic analysis performed for better describing the tidal current characteristics in the Bohai Sea, and promoting numerical modeling with more test data.

2 DATA AND METHODOLOGY

2.1 Data description

Tidal currents data in 11 stations of the Bohai Sea were analyzed. Fig.1 shows that the stations were evenly distributed all over the area. All the data were obtained in August or September in history and the description of them are shown in Table 1. In addition, two different devices, Acoustic Doppler Current Profiler (ADCP) and Direct Reading Current Meter (DRCM) were used at station A9. Long-term tidal currents were observed at station A11 for about 1 month. The observation interval at stations A1-A8 except A6 was 1 hour, read three times, continually, and averaged for bias-free, while for others only once.

2.2 Data preparation

A filter was required at the first step, since the direction of the current observed by DRCM was unsteady during a weak current period. The interval of recording was 1 h. Every three records at each period were averaged for stations A1, A2, A3, A4, A5, A7 and A8. Considering the discontinuity data sets resulted from device malfunction and/or harsh

weather, the approach to filling the gaps are described as:

(a) For short-term data (taking one day or many days as an example)

If the blank is within a few hours, simply insert a value according to the trend; otherwise, if the gap is < 12 h, a two-order parabola method is used (Fang et al., 1986). The data absent can be calculated using the formula:

$$U(t) = \frac{2}{3}[h(t-25) + h(t+25)] -$$
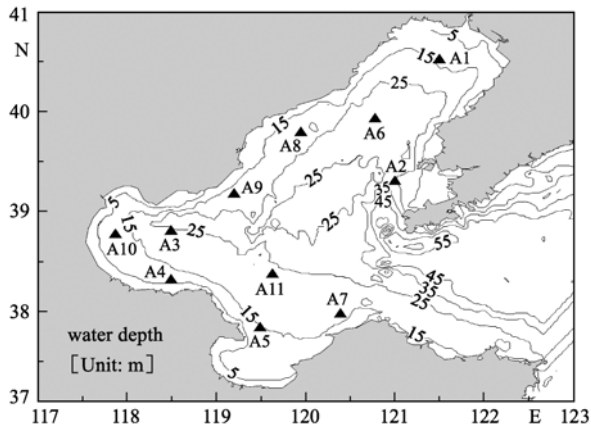$$\frac{1}{6}[h(t-50) + h(t+50)]$$

Fig.1 Distribution of the stations and isobath curves in the Bohai Sea

If the gap is >12 h in one day, or the initial value of the above method is difficult to estimate, the data of that day is discarded.

(b) For mid-term data (for example, the one-month long observation at station A11)

If the absent data is within 24 h, the method is the same as in (a). Otherwise, an iterative method is used. The initial value of discontinuous data is estimated by a data set of 15 days before or after. Then a harmonic analysis is carried out and the results are used to predict the absent data. Then the

harmonic analysis is conducted again. This process is repeated until the estimates of the absent data differ by less than a small value.

2.3 Harmonic analysis

With monthly harmonic analysis method, 46 major tidal constituents and 28 minor ones of the northern and eastern components of the tidal currents have been previously calculated from the monthly data sets (Fang et al., 1986).

For short-term observations, taking daily one as an example, quasi-harmonic analysis was used. The diurnal and semi-diurnal constituents were incorporated into four tidal current components of O_1, K_1, M_2, and S_2. And shallow water constituents M_4 and MS_4 were also taken into account. The harmonic constants of long-term observation station was introduced into the calculation of so-called "difference-ratio coefficient" (Fang, 1974).

3 RESULTS COMPARISON

3.1 Comparison in different durations

As we all know, it is difficult to get midterm or long-term tidal currents observation data. Therefore quasi-harmonic analysis data set in length of several days becomes more valuable.

To compare the harmonic results between a day and a month, the data set of station A11 were calculated. The quasi-harmonic and monthly harmonic analyses of daily and monthly data were conducted, respectively. As shown in Table 2, taking component M_2 as an example, the results of a full moon day and new-moon day are very close to the results from a monthly data. However, constants calculated from the first and last quarter-moon day deviate from the monthly result.

Table 1 Observation data description

Station	Duration	Device	Interval	Vertical level
A1	20000830-20000906		1 h	Surface, midlevel, bottom
A2	20000902-20000904		1 h	Surface, midlevel, bottom
A3	20000812-20000820	DRCM	1 h	Surface, midlevel, bottom
A4	20000812-20000820		1 h	Surface, midlevel, bottom
A5	20000812-20000820		1 h	Surface, midlevel, bottom
A6	19970815-19970825	Aanderaa current meter	20 min	5 m, 15 m, 30 m level
A7	20000812-20000819		1 h	Surface, midlevel, bottom
A8	20000901-20000908	DRCM	1 h	Surface, midlevel, bottom
A9	20010803-20010818	ADCP	15 min	14 m, 17 m level
	20010729-20010818	DRCM	1 h	10 m, 17 m level
A10	19980827-19980831	Aanderaa current meter	20 min	Surface level
A11	19960801-19960830	Aanderaa current meter	20 min	5 m, 18 m level

Therefore, if observation is within one month, the harmonic results from the Syzygy day can be used, especially the full-moon day. On the other hand, to get more accurate results, good weather conditions and multiple records are preferred.

3.2 Comparison in different devices

The ADCP is a relatively new device for current observation in acoustic Doppler principles to measure the vertical section of a tidal current. It has been developed since 1980s, featuring the convenience, high accuracy, and high resolution.

The SLC9-2 DRCM used in this research was developed by the Ocean University of China in 1980s for convenience and wide application.

The two devices were used at station A9. The harmonic analysis results are shown in Table 3. Along the major direction of movement, amplitudes of M_2 and S_2 constituents measured with DRCM are much larger, while the difference in phase lag is smaller than those of ADCP. However, for normal to major movement direction, the difference in phase lag is larger, which might be caused by the instability of the DRCM during weak currents.

Table 2 Harmonic constants of M_2 component current at station A11[*]

| Dataset type | M_2 tidal constituent | | | | | | | |
| | Surface Level | | | | Bottom Level | | | |
	H_u (cm/s)	G_u (°)	H_v (cm/s)	G_v (°)	H_u (cm/s)	G_u (°)	H_v (cm/s)	G_v (°)
New-moon day	23.88	50.46	33.73	180.77	20.25	20.18	28.61	163.58
Full-moon day	22.72	46.94	32.46	175.22	16.11	19.00	27.95	161.24
Monthly data	20.52	46.04	31.85	176.86	16.87	15.91	25.89	156.87
Results by Lou et al. (2002)	18.81	48.26	28.55	178.34	---	---	---	---
The last quarter day	22.11	27.65	32.46	164.09	17.02	9.77	28.04	145.18
The first quarter day	23.63	29.54	28.87	155.15	20.02	9.12	22.73	145.69

[*]H_u, C_u: amplitude and phase lag of northern current component, H_v, G_v amplitude and phase lag of eastern current component

Table 3 Harmonic results taken with different devices[*]

| Station A9 | M_2 tidal current component | | | | S_2 tidal current component | | | |
	H_u (cm/s)	G_u (°)	H_v (cm/s)	G_v (°)	H_u (cm/s)	G_u (°)	H_v (cm/s)	G_v (°)
ADCP	15.73	142.00	36.85	154.37	4.72	220.00	11.06	232.37
DRCM	14.38	128.90	41.95	159.34	4.31	206.89	12.59	237.34

[*]H_u, C_u: amplitude and phase lag of northern current component, H_v, G_v amplitude and phase lag of eastern current component

4 CHARACTERISTICS OF TIDAL CURRENT

4.1 Harmonic constant

The northern and eastern components of the harmonic constants of 11 stations in the Bohai Sea were calculated (Table 4). Apparently, M_2 is the major constituent, while in some area, such as station A2 that located west of the peninsula; K_1 and O_1 occupied a large proportion of tidal currents.

4.2 Characteristics of tidal current

Based on the northern and eastern components of harmonic constants of tidal currents, tidal ellipses were calculated.

The surface situation of M_2 tidal currents is shown in Fig.2. The rotation direction at stations A1, A4, and A10 was anti-clockwise, while clockwise at stations A5, A7, and A11. At the bottom level (Fig.3), major semi-axis, i.e. maximum tidal speed, of M_2 tidal current component was smaller than the

surface one. The rotation direction at stations A1, A3, A4, A5, A7 and A11 are the same as those at the surface. However, the rotation direction at station A8 off Qinhuangdao City changed from clockwise at surface to anti-clockwise at bottom, which might be resulted from the increasing of ellipticity k in vertical direction, which has been explained in relevant theory by Fang (1984). In addition, the tidal current at station A6 featured to-and-fro styled current.

Compared to component M_2, the surface major semi-axis of K_1 was much smaller as shown in Fig. 4. The rotation direction at almost all the stations was clockwise, except for stations A4 and A5. The back-and-forth currents can be found at stations A1, A6, A10, and A11. The velocity of the bottom K_1 tidal current was very small (Fig.5). Based on the ellipticity k of the tidal ellipse, the rotation direction at all the stations was anti-clockwise except for stations A2 and A8, and those at stations A6, A7, and A11 were opposite to the surface.

Table 4 Harmonic constants of currents at 11 stations*

O$_1$	Surface				Mid level				Bottom			
	H_u (cm/s)	G_u (°)	H_v (cm/s)	G_v (°)	H_u (cm/s)	G_u (°)	H_v (cm/s)	G_v (°)	H_u (cm/s)	G_u (°)	H_v (cm/s)	G_v (°)
A1	5.12	133.60	4.19	6.85	4.36	349.41	4.58	224.91	2.74	351.96	4.12	306.92
A2	41.68	291.99	40.81	38.90	15.94	197.06	6.35	272.40	14.07	180.11	10.50	227.73
A3	6.79	60.34	16.31	170.03	3.96	246.53	9.15	225.53	4.14	237.69	6.18	211.93
A4	4.40	218.87	4.54	167.11	3.98	214.20	2.62	148.10	2.83	215.80	1.715	154.90
A5	8.96	282.51	6.29	215.46	6.72	270.54	2.12	164.26	5.78	266.30	2.37	191.34
A6	4.62	289.15	7.44	293.17	4.77	330.05	6.64	298.29	6.33	334.76	6.61	310.42
A7	3.93	77.08	22.57	185.28	6.16	227.22	10.94	197.55	5.26	232.18	8.38	193.79
A8	3.57	105.44	7.18	227.31	7.18	299.27	6.17	169.15	7.17	133.23	9.90	231.19
A9	---	---	---	---	---	---	---	---	7.38	258.00	6.74	206.96
A10	1.63	221.97	5.42	204.35	---	---	---	---	---	---	---	---
A11	6.32	13.94	8.73	189.43	---	---	---	---	4.16	53.37	13.37	204.91

K$_1$	Surface				Mid level				Bottom			
	H_u (cm/s)	G_u (°)	H_v (cm/s)	G_v (°)	H_u (cm/s)	G_u (°)	H_v (cm/s)	G_v (°)	H_u (cm/s)	G_u (°)	H_v (cm/s)	G_v (°)
A1	7.02	62.59	5.75	51.19	5.97	52.7	6.28	33.91	3.75	40.96	5.65	175.92
A2	59.54	334.99	58.30	81.90	22.78	60.06	9.07	135.40	20.10	223.11	15.00	270.73
A3	9.05	102.34	21.75	212.03	5.28	288.53	12.20	267.53	5.52	279.69	8.25	253.93
A4	6.16	263.87	6.36	212.11	5.58	259.20	3.67	193.10	3.96	260.80	2.40	199.90
A5	13.44	330.51	9.44	263.46	10.07	318.54	3.1	212.26	8.67	314.39	3.56	239.34
A6	6.84	334.15	11.03	338.1	7.07	25.90	9.84	331.46	9.37	31.38	9.79	346.96
A7	6.55	127.08	37.62	235.28	10.26	277.22	18.23	247.55	8.76	282.	13.96	243.79
A8	5.00	147.44	10.05	269.31	10.06	341.27	8.63	211.15	10.04	175.23	13.86	273.19
A9	---	---	---	---	---	---	---	---	9.84	300.00	8.99	248.96
A10	2.18	255.97	6.46	251.95	---	---	---	---	---	---	---	---
A11	7.03	49.87	14.22	224.70	---	---	---	---	3.22	52.74	16.52	238.84

M$_2$	Surface				Mid level				Bottom			
	G_u (°)	H_v (cm/s)	G_v (°)	H_u (cm/s)	G_u (°)	H_v (cm/s)	G_v (°)	H_u (cm/s)	G_u (°)	H_v (cm/s)	G_v (°)	H_u (cm/s)
A1	37.46	76.54	43.53	72.37	35.51	75.93	38.28	68.27	32.76	75.97	32.67	62.97
A2	68.24	19.04	11.24	60.73	65.86	8.59	18.83	21.31	49.47	2.49	17.42	353.68
A3	7.75	72.47	59.68	200.57	5.62	246.91	65.09	190.04	12.35	276.44	52.33	179.41
A4	22.58	249.21	67.78	191.30	22.59	240.18	59.63	188.53	19.88	228.98	47.99	192.46
A5	64.68	108.01	19.21	167.33	57.02	89.58	16.20	167.32	47.37	86.65	10.71	170.11
A6	23.88	55.17	35.69	62.3	16.90	45.37	33.08	55.99	24.50	50.28	27.85	39.25
A7	23.47	142.04	56.64	193.80	7.60	77.61	47.59	159.90	6.13	75.55	39.99	155.97
A8	11.04	76.34	17.02	101.74	11.78	92.53	22.04	98.07	12.37	104.06	12.37	96.92
A9	---	---	---	---	---	---	---	---	15.73	142.00	36.85	154.37
A10	12.17	224.13	27.86	190.35	---	---	---	---	---	---	---	---
A11	20.11	45.51	31.13	176.50	---	---	---	---	16.85	15.46	25.88	156.52

| S$_2$	Surface				Mid level				Bottom			
	G_u (°)	H_v (cm/s)	G_v (°)	H_u (cm/s)	G_u (°)	H_v (cm/s)	G_v (°)	H_u (cm/s)	G_u (°)	H_v (cm/s)	G_v (°)	H_u (cm/s)
A1	10.76	130.54	12.50	126.37	10.20	129.93	10.99	122.27	9.41	129.97	9.38	116.97
A2	20.89	75.09	3.44	116.73	20.16	64.59	5.76	77.31	15.14	58.49	5.33	49.68
A3	2.29	149.47	17.61	277.57	1.66	323.9	19.21	267.04	3.65	349.43	15.44	256.41
A4	4.46	326.21	13.38	268.30	4.46	317.18	11.77	265.53	3.92	305.98	9.47	269.46
A5	12.66	185.01	3.76	244.33	11.16	166.58	3.17	244.32	9.27	163.65	2.10	247.11
A6	5.87	112.17	8.78	119.39	4.16	102.37	8.14	112.99	6.03	107.28	6.85	96.25
A7	4.59	220.04	11.08	271.80	1.49	155.61	9.31	237.90	1.20	153.55	7.82	233.97
A8	4.25	154.34	6.54	179.74	4.53	170.53	8.48	176.07	4.76	182.06	4.76	174.92
A9	---	---	---	---	---	---	---	---	4.72	220.00	11.06	232.37
A10	2.63	301.13	6.03	267.35	---	---	---	---	---	---	---	---
A11	4.79	122.34	7.38	236.41	---	---	---	---	4.29	89.10	7.23	214.42

* The surface, mid, and bottom levels are relative levels of different water depths at different stations; the results of A9 was calculated by data observed with ADCP. H_u, C_u: amplitude and phase lag of northern current component, H_v, G_v amplitude and phase lag of eastern current component
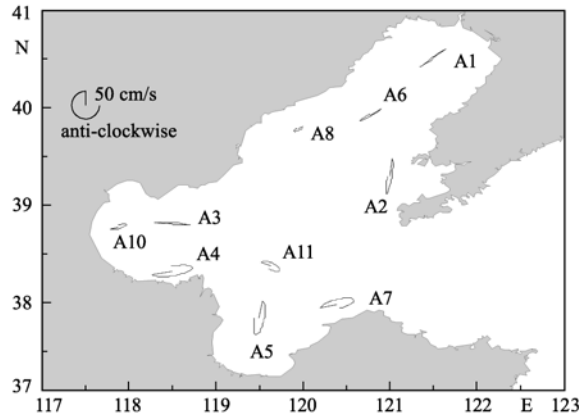
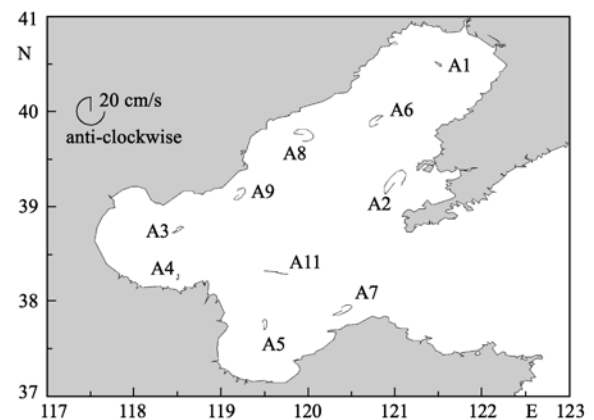**Fig.2 The current ellipses of M$_2$ tidal current at surface level, of which semi-axis and rotation directions are shown. The non-closed ellipses indicate the rotation direction of tidal current**
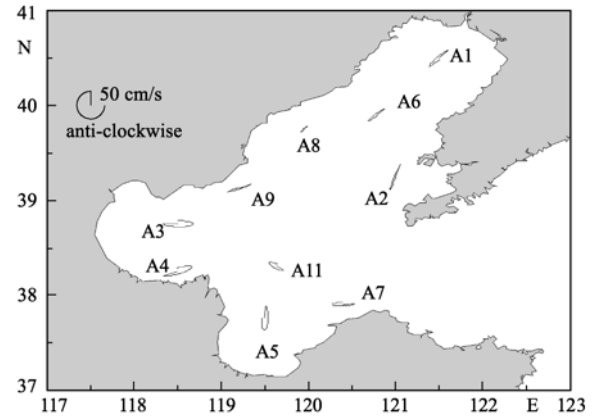
Fig.3 The current ellipses of M$_2$ tidal current at bottom level, of which semi-axis and rotation directions are shown
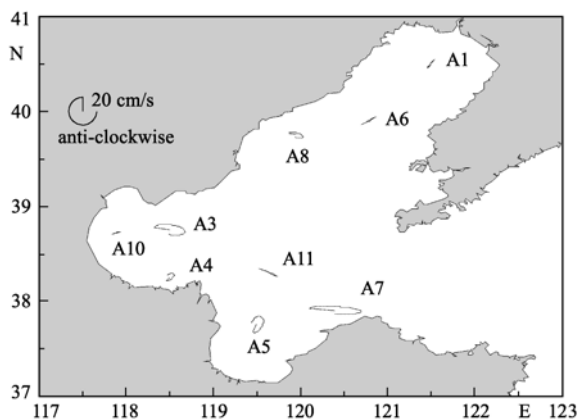
Fig.4 The current ellipses of K$_1$ tidal current at surface level, of which semi-axis and rotation directions are shown

Fig.5 The current ellipses of K$_1$ tidal current at bottom level with semi-axis and rotation directions shown

The observed results described above are in agreement with previous two-dimensional modeling studies (Fang, 1984, Huang, 1991), except for surface layer at station A3 for M$_2$ and at station A3, A7 and A8 for K$_1$ tidal ellipses. The difference in rotation direction at those stations may have been caused by integration of the two-dimensional model, while it is three-dimensional in the field observation.

4.3 Property of tidal current

According to the criterion $HR=(W_{O_1}+W_{K_1})/W_{M_2}$, the characteristics of tidal currents are shown in Table 5. W_C (C=O$_1$, K$_1$, M$_2$, S$_2$, M$_4$, MS$_4$) stands for the maximum speed of tidal current constituent. If $HR \leq 0.5$, that is regular semi-diurnal tidal current; else if $0.5 < HR \leq 2.0$, irregular semi-diurnal tidal current; else if $2.0 < HR \leq 4.0$, irregular diurnal tidal current; otherwise, regular diurnal.

The summer observation results show that it was a regular semi-diurnal tidal current at station A1 in the Liaodong Bay, A3, A4, and A10 in the Bohai Bay, and A5 in the Laizhou Bay, which is consistent

with Huang's (1991) report. The observations in the stations A2, A6, A7, A8, A9, and A11 were irregular semi-diurnal tidal current, while it was different at station A3 from the surface to bottom probably due to the faster variation in the maximum speed of the diurnal tidal current ($W_{O_1}+W_{K_1}$) than that of the semi-diurnal tidal current (W_{M_2}) in vertical direction (Fang, 1984).

4.4 Vertical distribution of maximum speed

Fig.6 illustrates the vertical variation of the maximum speed, i.e. the major semi-axis of the tidal ellipse of the diurnal and semi-diurnal tidal current.

In general, an hourly record may cause some errors in calculating the maximum speed; however, the trend of vertical variation is more reliable at least.

Both diurnal and semi-diurnal tidal currents, the maximum speed at 7 stations decreased gradually surface to bottom resulted from bottom friction (Fig.6). However, the direction of maximum tidal current remains unchanged.

Table 5 Characteristics of tidal currents in the 11 stations

| Station | HR value | | | Type of tidal current |
	Surface	Mid level	Bottom	
A1	0.26	0.27	0.24	Regular semi-diurnal tidal current
A2	1.65	0.57	0.75	Irregular semi-diurnal tidal current
A3	0.64	0.35	0.32	Irregular semi-diurnal tidal current in surface
				Regular semi-diurnal tidal current at bottom
A4	0.20	0.16	0.14	Regular semi-diurnal tidal current
A5	0.36	0.30	0.31	Regular semi-diurnal tidal current
A6	0.51	0.51	0.58	Irregular semi-diurnal tidal current
A7	1.03	0.69	0.63	Irregular semi-diurnal tidal current
A8	0.90	0.83	1.37	Irregular semi-diurnal tidal current
A9	---	---	0.53	Irregular semi-diurnal tidal current
A10	0.42	---	---	Regular semi-diurnal tidal current
A11	0.77	---	1.04	Irregular semi-diurnal tidal current
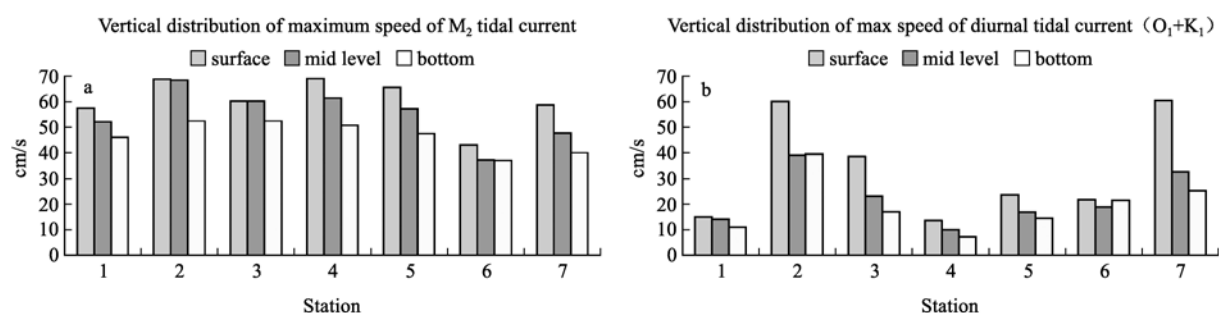
Fig.6 Maximum speeds of (a) semi-diurnal and (b) diurnal tidal current at the surface, mid level and bottom

5 CONCLUSION

With harmonic analysis method, the characteristics of tidal currents observed in summer for the Bohai Sea were studied. After comparing the data processed, harmonic constants of Syzygy day, especially the full-moon day was chosen for use instead of those from the monthly data if the duration of recording was short.

The rotation direction of M_2 tidal current component was clockwise in the Laizhou Bay and the central Bohai Sea, while anti-clockwise in the Liaodong Bay and other areas of the Bohai Bay in both surface and bottom layers. For that of K_1 component, it was clockwise at surface in the central Bohai Sea but anti-clockwise in that of the Laizhou Bay and Liaodong Bay, similarly for the bottom. The rotation direction of the K_1 in the Bohai Bay changed from clockwise at the surface to anti-clockwise at the bottom.

There were regular semi-diurnal tidal currents in the Liaodong Bay and Bohai Bay, while irregular semi-diurnal tidal currents in the central part of the Bohai Sea.

The maximum speed of the K_1 component was much smaller than that of M_2, and both K_1 and M_2 decreased from the surface to the bottom. The vertical variation in maximum speed direction was not obvious.

6 ACKNOWLEDGMENT

References

Bao, X. W., J. Yan and W. X. Sun, 2000. A three-dimensional tidal model in boundary-fitted curvilinear grids. *Estuarine Coastal and Shelf Science* **60**: 775-788.

Chen, Z. Y., 1980. Tide. Science Press, Beijing, China. pp. 1-301. (in Chinese)

Dou, Z. X., L. W. Yang and J. Ozer, 1993. A three-dimensional model for the simulation of tide and tidal currents in Bohai. *ACTA Oceanol. Sinica.*15: 1-15.

Fang, G. H., 1974. Quasi-harmonic constituent method for analysis and prediction of tides．*Stadia Marines Sinica.* **9**: 1-15. (in Chinese)

Fang, G. H., 1984. Basic characteristics of the vertical

structure of tidal currents-A comparison of theory and observations. *Marin Science*. **3**: 1-11. (in Chinese)

Fang, G. H. and J. F. Yang, 1985. A 2-D numerical model of tide in Bohai Sea. *Oceano1. et Limno1. Sin.* **16**(5): 337-346. (in Chinese with English abstract)

Fang, G. H., W. Z. Zheng, Z. Y. Chen and J. Wang, 1986. Analysis and Prediction of Tide and Tidal Currents. Ocean Press, Beijing, China. pp.1-474. (in Chinese)

Huang, Z. K., 1991. Tidal waves in the Bohai Sea and their variations. *Journal of Ocean University of Qingdao*. **21**(2): 1-11. (in Chinese with English abstract)

Huang, D., J. Su and J. O. Backhaus, 1999. Modeling the seasonal thermal stratification and baroclinic circulation in the Bohai Sea. *Continental Shelf Research* **19**(11): 1 485-1 505.

Kuang, G. R., Q. Zhang and Y. Z. Dai, 1991. Observation of long-term currents and analysisi of residual currents in central Bohai Sea. *Transactions of Oceanology and Limnology.* **2**: 1-11. (in Chinese)

Li, G. S., H. L. Wang and B. L. Li, 2005. A model study on seasonal spatial-temporal variability of the Lagrangian Residual Circulations in the Bohai Sea. *Journal of Geographical Sciences* **15**(3): 273-285.

Lou, A. G., X. C. Wang, D. X. Wu, H. P. Li and W. Chang, 2002. Analysis of one month's current data observed in middle of Bohai Sea. *Marine Science* **26**(11): 23-27. (in Chinese with Enlgish abstract)

Shi, M. C., G. P. Gao and X. W. Bao, 2000. Marine Investigation Methods. Ocean University of China Press, Qingdao, China. pp. 1-343. (in Chinese)

Wan, X. Q., X. W. Bao, D. X. Wu, X. S. Guo and H. Jiang, 2003. Numerical simulation of the tidal currents and the pollutant diffusion in Jiaozhou Bay. *Marine Science* **27**(5): 41-47. (in Chinese with abstract)

Wei, H., D. Hainbucher, T. Pohlmann, S. Z. Feng and J. Suendermann, 2004. Tidal-induced Lagrangian and Eulerian mean circulation in the Bohai Sea. *Journal of Marine Systems* **44**(3-4): 141-151.

Wu, D. X., X. Q. Wan, X. W. Bao, L. Mu and J. Lan, 2004. Comparison of summer thermohaline field and circulation structure of the Bohai Sea between 1958 and 2000. *Chinese Science Bulletin* **49**(4): 363-368.

Yu, J. H., J. F. Zhao and Y. G. Zhang, 2002. Characteristics of tidal current of the northern mouth of Dalian Bay near the coast. *Marine Science Bulletin* **21**(6): 25-30. (in Chinese)